INFECTION AND IMMUNITY, Dec. 2000, p. 7166–7171 Vol. 68, No. 12
0019-9567/00/$04.00+0

fbpABC Gene Cluster in *Neisseria meningitidis* Is Transcribed as an Operon

HENG H. KHUN,[1] VINAY DEVED,[1] HOWARD WONG,[2] AND B. CRAIG LEE[1]*

Department of Microbiology and Infectious Disease, University of Calgary, Calgary, Alberta, Canada T2N 4N1,[1] and Department of Pathology and Laboratory Medicine, Calgary Laboratory Services, Foothills Medical Centre, Calgary, Alberta, Canada T2N 2T9[2]

Received 30 June 2000/Returned for modification 11 August 2000/Accepted 15 September 2000

The neisserial *fbpABC* locus has been proposed to constitute a single transcriptional unit. To confirm this operonic arrangement, transcription assays using reverse transcriptase PCR amplification were conducted with *Neisseria meningitidis*. The presence of *fbpAB* and *fbpBC* transcripts obtained by priming cDNA synthesis with an *fbpC*-sequence-specific oligonucleotide indicates that *fbpABC* is organized as a single expression unit. The ratio of *fbpA* to *fbpABC* mRNA was approximately between 10- to 20-fold, as determined by real-time quantitative PCR.

The necessity to sequester essential biochemical processes poses a challenge for living cells. Physical compartmentalization created by semipermeable membrane partitions achieves this segregation, but at the predictable expense of imposing a restrictive barrier to the cellular ingress and exit of solutes. Prokaryotes and eukaryotes have surmounted this obstacle by evolving transport systems, termed ATP-binding cassette (ABC) transporters, that couple ATP hydrolysis with substrate translocation across biological membranes (2, 6, 12, 24). These systems exhibit a modular organization comprised of four structural domains that may be expressed as individual polypeptides or may be fused into single multidomain proteins. Two membrane-integral domains span the membrane multiple times and form the passageway through which the solute flux occurs. Two ATP-binding cassettes reside on the cytosolic face of the membrane.

The binding-protein-dependent transporters of gram-negative bacteria represent the best-characterized members of this superfamily. These transporters recruit an auxiliary component, a periplasmic binding protein, that constitutes the major determinant in conferring substrate specificity (2, 6, 7, 12, 20, 26). The genes encoding this transporter complex are arranged as a single transcriptional unit, although apparent exceptions exist in which the periplasmic binding protein genes are unlinked from their cognate permease genes (8, 15, 23).

In the pathogenic neisseria *Neisseria gonorrhoeae* and *Neisseria meningitidis*, a gene cluster, termed *fbpABC*, has been postulated to mediate the delivery of iron across the periplasmic space into the cytoplasm (1, 5). The iron acquisition phenotype of a meningococcal *fbpABC* mutant supports this proposal for the obligatory participation of *fbpABC* in neisserial periplasmic iron transport from human transferrin and human lactoferrin (14). This locus displays the signature core components characteristic of binding-protein-dependent ABC transporters. Biochemical studies (5) identify FbpA as the substrate binding protein. The functional assignments of FbpB as the cytoplasmic membrane protein and of FbpC as the ATPase subunit are implied by the deduced amino acid sequence similarity to homologous proteins (1).

It remains unclear whether the genes in this locus are cotranscribed as a single expression unit. Nucleotide sequence (1) and primer extension (9) analyses have mapped a single potential promoter site upstream of *fbpA*. However, Northern blot hybridization did not disclose the presence of a polycistronic transcript (9). Therefore, this investigation was undertaken to address the proposed operonic organization of *fbpABC* by conducting transcription assays that exploit the sensitivity of reverse transcriptase (RT)-PCR amplification.

Bacterial strains and growth conditions. The bacteria used in this study are listed in Table 1. Neisserial strains were grown on chocolate agar at 35°C in an atmosphere of 5% CO_2. A single colony was selected from overnight growth on chocolate agar to inoculate 10 ml of brain heart infusion (BHI) broth (Difco Laboratories, Detroit, Mich.) containing a 50 μM concentration of the iron chelator EDDA [ethylenediamine-di(*o*-hydroxyphenylacetic acid)]. The culture was grown in a shaking incubator at 37°C in the presence of 5% CO_2 until mid-logarithmic growth was achieved (equivalent to an optical density at 600 nm [OD_{600}] of 0.685 as measured with a Pye Unicam PU8800 spectrophotometer).

DNA isolation and manipulations. Meningococcal genomic DNA was recovered by standard methods (21). DNA fragments were purified from agarose gels by using either the GeneClean II Purification Matrix kit (BIO 101, Inc., Vista, Calif.) or by passage through NENSORB 20 (NEN, Boston, Mass.) cartridges. DNA sequencing was performed according to the dideoxynucleotide chain-termination method (22) with a PRISM Ready Reaction dye cycle sequencing kit (Applied Biosystems) with fluorescence-labelled synthetic oligonucleotide primers based on the known *fbpABC* sequence (1). All sequence reactions were run and analyzed on an Applied Biosystems 377XL automated DNA sequencer.

The *fbpABC* locus from *N. meningitidis* B16B6 chromosomal DNA was PCR amplified with primer set 5′fbpA and 3′fbpCstop with *Pfu* DNA polymerase (Stratagene, La Jolla, Calif.). The amplification product was ligated into the TA cloning vector pCR2.1 (Invitrogen, San Diego, Calif.), creating pCR2FABC. This construct was used to generate the standard curves in the quantitative PCR assay.

* Corresponding author. Present address: Division of Infectious Diseases, Department of Medicine, University of Ottawa, 501 Smyth Rd., Ottawa, Ontario, Canada K1H 8L6. Phone: (613) 737-8880. Fax: (613) 737-8925. E-mail: clee@uottawa.ca.

TABLE 1. Bacterial strains, plasmids, and primers used in this study

Strain, plasmid, or primer	Relevant characteristic(s)	Source or reference
Strain		
Neisseria meningitidis B16B6	Clinical isolate, serogroup B, serotype 2a	C. Frasch
Plasmids		
PCR2.1	TA cloning vector, ampicillin and kanamycin resistance	Invitrogen
pCR2FABC	PCR2.1 containing the cloned *fbpABC* locus from *N. meningitidis* B16B6	This study
Primers (5′→3′)		
5′fbpA	CA**GCCGTCTGAA**AGGAATACACTACACCCG; 5′ oligonucleotide containing the gonococcal uptake sequence (boldface) for the amplification of *fbpABC*, nucleotide positions 45–70[a]	14
5′fbpAint	GTACAAAATGTCCACACCCGC; 5′ oligonucleotide for the amplification of *fbpAB*, nucleotide positions 801–821[a]	This study
3′fbpBint	CAGGCTGATGCGTTTGAGTGC; 3′ oligonucleotide for the amplification of *fbpAB*, nucleotide positions 1600–1620[a]	This study
5′fbpBint	CCTTTATCGTCGTCATCCTT; 5′ oligonucleotide for the amplification of *fbpBC*, nucleotide positions 2321–2340[a]	This study
3′fbpCint	CGGACGGGAAGGTTGGTATT; 3′ oligonucleotide upstream of the Walker A motif for the amplification of *fbpBC*, nucleotide positions 2939–2959[a]	This study
3′fbpCstop	TGCCGCCTT**TCA**GAGGGTATTTCC; 3′ oligonucleotide reverse primer encompassing the stop codon (boldface) of *fbpC*, nucleotide positions 3771–3794[a]	This study
5′HKasdint	GTATCTGATTTCCTGCGCAGCG; 5′ oligonucleotide for the amplification of *asd*, nucleotide positions 8290–8311[b]	This study
3′HKasdstop	GC**TTA**CAGGCTGCCCAACACG; 3′ oligonucleotide encompassing the stop codon (boldface) for the amplification of *asd*, nucleotide positions 8769–8798[b]	This study
48	TTCTGCATTCCTTATGCGCATGGATTTC; 3′ oligonucleotide for the amplification of *tbpA*, nucleotide positions 560–575[c]	This study
385	AAATTTGGATCCGAAAGCGAAGATTAG; 5′ oligonucleotide for the amplification of *tbpA*, nucleotide positions 1940–1965[c]	This study
560	CCATGCATCATTTAGGAGGAAATCGATA**TG**; 5′ oligonucleotide containing the Shine-Dalgarno sequence (underlined) and the start codons (boldface) for the amplification of *fbpA*, nucleotide positions 100–122[a]	This study
561	ATCCGATGCATGC**TTA**TTTCATACCGGCTTG; 3′ oligonucleotide upstream of the stem-loop structure (boldface type indicates the stop codon) for the amplification of *fbpA*, nucleotide positions 1098–1117[a]	This study

[a] The positions correspond to the nucleotide sequences of *fbpABC* (EMBL/GenBank DDBJ Nucleotide Sequence Data Library accession no. U33937) (1).
[b] The positions correspond to the nucleotide sequences of *asd* (EMBL/GenBank DDBJ Nucleotide Sequence Data Library accession no. AE002557).
[c] The positions correspond to the nucleotide sequences of *tbpA* (EMBL/GenBank DDBJ Nucleotide Sequence Data Library accession no. Z15129).

RNA isolation and RT-PCR. Total cellular RNA was extracted from mid-logarithmic-phase (OD_{600} of 0.685) meningococcal cultures by using the RNeasy Midi kit (Qiagen, Inc., Clarita, Calif.) according to the manufacturer's recommendations. To eliminate contaminating genomic DNA, total RNA was subjected to DNase I (amplification grade, Gibco BRL, Life Technologies, Burlington, Canada) treatment as specified by the manufacturer. RNA concentrations were determined by measuring the A_{260}; samples were immediately stored at −70°C. Reverse transcription was performed with the SuperScript II RNase H^- RT-PCR kit (Gibco BRL) following the manufacturer's instructions. The indicated gene-specific primers (Table 1) initiated first-strand cDNA synthesis. Thirty-six cycles of PCR amplification were performed with *Taq* polymerase (Gibco BRL) on a Perkin-Elmer model 480 DNA thermal cycler with denaturation at 94°C for 30 s, primer annealing at 52°C for 30 s, and extension at 72°C for 3 min. Identical aliquots were processed in parallel without the addition of RT, in order to ensure that residual genomic DNA was not serving as the template in the PCR amplification. PCR amplification products were electrophoresed on 1% agarose gels and stained with ethidium bromide. The identity of all RT-PCR amplification fragments was verified by nucleotide sequencing.

QRT-PCR. For quantitative RT-PCR (QRT-PCR), cDNA synthesis was performed in a 20-μl final volume that included 2 μg of meningococcal total RNA, 100 pmol of random hexamer oligonucleotides (N6) as primers, RT buffer (50 mM Tris [pH 8.3], 75 mM KCl, 1.5 mM $MgCl_2$), 10 mM dithiothreitol, and 1 mM (each) deoxynucleoside triphosphates (dNTPs; dATP, dGTP, dCTP, and dTTP), 100 U of Superscript II RT (Gibco BRL), and 17 U of RNase inhibitor (RNAguard; Am-

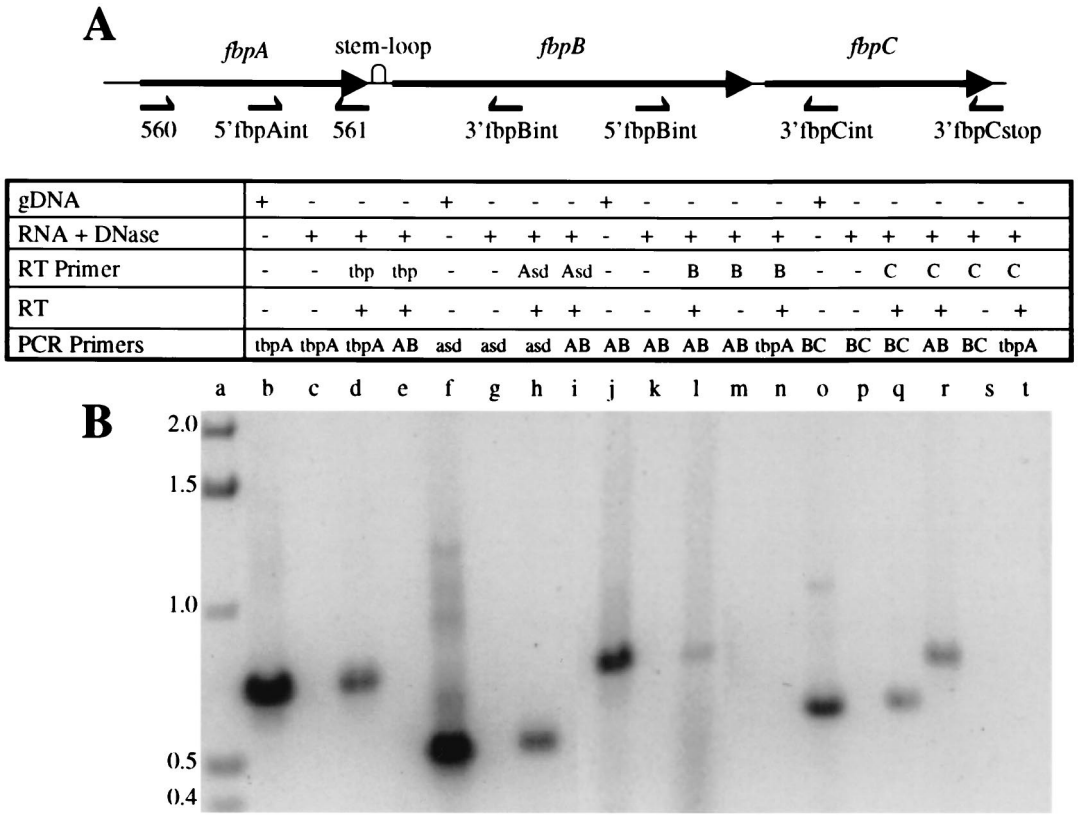

FIG. 1. (A) The meningococcal *fbpABC* gene cluster encoding the neisserial iron ABC transporter. The orientations and approximate positions of the gene-specific primers for generating the cDNA and the oligonucleotide primers used in the PCR amplification step of the RT-PCR assays are displayed below the schematic. gDNA, genomic DNA. (B) RT-PCR amplification of total RNA extracted from *N. meningitidis* B16B6. The PCR amplification products were fractionated in a 1% agarose gel that was stained with ethidium bromide. The ingredients used to generate the amplicon in each lane are depicted in the table above the agarose gel. RT primers are designated as follows: tbp, 48; Asd, 3′HKasdstop; B, 3′fbpBint; and C, 3′fbpCstop. PCR primer pairs are designated as follows: tbpA, 385 and 48; asd, 5′HKasdint and 3′HKasdstop; AB, 5′fbpAint-3′fbpBint; and BC, 5′fbpBint-3′fbpCint. The figure was imaged with a Hewlett-Packard ScanJet HP, edited by using Adobe Photoshop 3.0, and labelled by using Microsoft PowerPoint 97. The sizes of standards in kilobases (lane a) are shown on the left.

ersham Pharmacia Biotech, Inc., Baie d'Urfé, Canada). The RT reaction was performed in an MJ Research minicycler PTC-150 at 22°C for 5 min, followed by incubation at 4°C for 50 min. The samples were heated for 5 min at 95°C to terminate the reaction. Real-time quantitative PCR was performed in 10-μl final volumes in glass capillaries in a LightCycler Instrument (Roche Diagnostics, Laval, Canada) (29). The PCR master mix comprised 1× PCR buffer, 3 mM $MgCl_2$, 1 mg of bovine serum albumin per ml, 0.2 mM dNTPs, 0.5 μM both forward and reverse primers, a 1:3,000 dilution of SYBR Green I (Molecular Probes), and 0.4 U of Platinum *Taq* (Gibco BRL). Into each capillary tube, 9 μl of PCR master mix and 1 μl of template target DNA (cDNA or pCR2FABC) were loaded. Sealed capillaries were centrifuged prior to placement into the LightCycler carousel. PCR amplification was performed with an initial denaturation at 95°C for 30 s followed by 45 cycles of denaturation at 95°C for 2 s (ramping at 20°C/s), annealing at 52°C for 5 s (ramping at 20°C/s), and elongation at 72°C for 42 s (ramping at 5°C/s). Amplicon specificity was verified by melting curve analyses with the LightCycler software, version 3.39. The identity of the amplicons was also established by confirmation of the expected molecular weight by agarose gel electrophoresis. Optimal conditions for amplification were determined by preliminary experiments with meningococcal genomic DNA. The quantitative PCR experiment was repeated three times, and each experiment produced similar results.

Transcription assays using RT-PCR. The integrity of the total RNA preparation was assessed by demonstrating the presence of the transcript from the housekeeping gene *asd* (10) (Fig. 1B, lane h; gene-specific primer 3′HKasdstop for the RT step, primer pair 5′HKasdint and 3′HKasdstop for PCR amplification) and the presence of the iron-regulated transcript *tbpA* (Fig. 1B, lane d; gene-specific oligonucleotide 48 for the RT step, primers 385 and 48 for the PCR step). The latter result also suggests that the starting RNA preparation is unlikely to be selectively biased against iron-regulated transcripts. The requirement for such a representative mRNA library arises from two considerations. First, the transcription of *fbpA* is enhanced under iron-limiting conditions (9). Second, given the proposed operonic organization of *fbpABC*, the expression of the putative polycistronic transcript encompassing this gene cluster would be anticipated to exhibit the same property.

The RT-PCR strategy used in the transcription assays was based on the general premise that upstream gene sequences within a given transcript would be readily detected by PCR amplification if these regions formed a continuous message. First-strand synthesis was initiated with gene-specific primers designed to anneal to intragenic sites within *fbpB* or *fbpC* and to the region encompassing the *fbpC* stop codon. Primer pairs were then selected to bracket the intergenic junctions between *fbpAB* and *fbpBC* (Fig. 1A). PCR amplification products generated by these oligonucleotides would therefore be contiguous and would be derived from a polycistronic transcript.

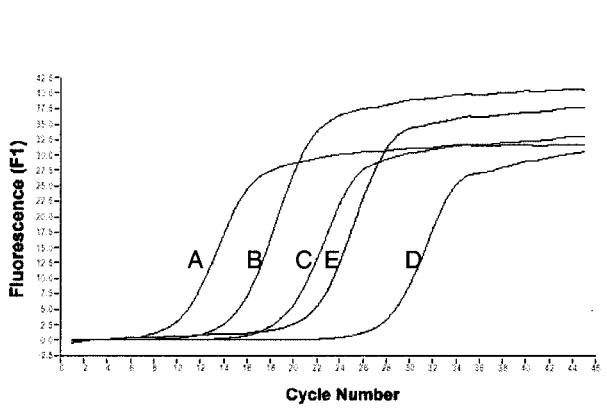

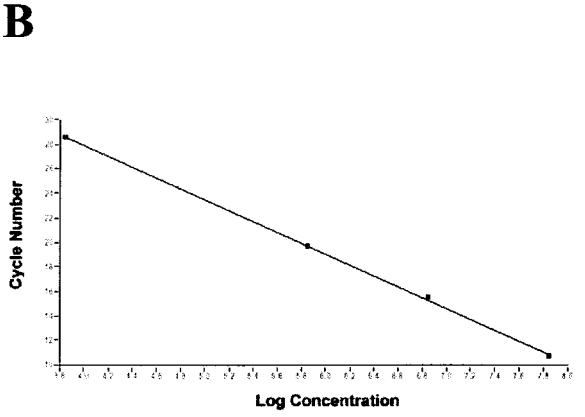

C

Primer pair	Template	Added copy number	Calculated copy number	C_t
560/561	pCR2FABC	70,000,000	76,150,000	10.72
560/561	pCR2FABC	7,000,000	6,172,000	15.56
560/561	pCR2FABC	700,000	714,500	19.71
560/561	pCR2FABC	7,000	7,150	28.58
560/561	Random hexamer primed cDNA	Unknown	195,100	22.21

FIG. 2. (A) Kinetic PCR curves for primer pair 560 and 561. Relative fluorescence output is plotted versus PCR cycle number. Kinetic curves are for 10^7 (A), 10^6 (B), 10^5 (C), and 10^3 (D) pCR2FABC DNA template copy numbers and for random-hexamer-primed cDNA (E). (B) Calibration curve for primer pair 560 and 561. The C_t value from each kinetic curve is plotted versus the log of the initial DNA concentration. (C) Copy number measured by real-time QRT-PCR. The copy number of standard pCR2FABC DNA added to the reactions is calculated from the moles of standard pCR2FABC added multiplied by Avogadro's number (6×10^{23}). Given the C_t of each sample, the initial copy number is calculated from the calibration curve conducted during the same experiment. Each assay was performed in triplicate, and representative data from one such experiment are shown. The figure was imaged with a Hewlett-Packard ScanJet HP, edited by using Adobe Photoshop 3.0, and labelled by using Microsoft PowerPoint 97.

Using a cDNA template reverse transcribed from primer 5′fbpBint engineered for sequences situated within *fbpB*, an amplicon spanning the *fbpAB* junction was detected (Fig. 1B, lane I; oligonucleotides 5′fbpAint and 3′fbpBint). This result indicates that *fbpA* and *fbpB* are cotranscribed.

Similarly, the presence of the predicted PCR fragments straddling the *fbpAB* (Fig. 1B, lane r; primers 5′fbpAint and 3′fbpBint) and *fbpBC* (Fig. 1B, lane q; primers 5′fbpBint and 3′fbpCint) intergenic regions, when cDNA generated from the *fbpC*-specific oligonucleotide 3′fbpCstop was used as template, indicates that *fbpA*, *fbpB*, and *fbpC* are cotranscribed. Thus, the aggregate RT-PCR data illustrate that *fbpABC* is organized as a single polycistronic transcriptional unit.

The results from a series of control experiments conducted concurrently with each of the four sets of RT-PCR assays confirmed the substrate quality and guaranteed the specificity of each component of the RT-PCRs. First, signals for the specific PCR products were lost when DNase I-treated total RNA served as the template (Fig. 1B, lanes c, g, k, and p), ensuring that residual genomic DNA had not contaminated the starting RNA preparations. Second, the presence of the expected amplicon when genomic DNA acted as the template (Fig. 1B, lanes b, f, j, and o) demonstrated the fidelity of the PCR primers. Third, the absence of a PCR product when reciprocal PCRs were primed with a heterologous oligonucleotide pair (Fig. 1B, lanes e, i, n, and t) verified the authenticity of the cDNA template generated by the gene-specific reverse primer. Last, the inability to PCR amplify the desired product when RT was omitted (Fig. 1B, lanes m and s) (data not shown) validated the compulsory requirement of this enzyme for the initiation of cDNA synthesis.

Transcript quantity. Real-time PCR studies were used to determine the relative abundance of *fbpA*-, *fbpAB*-, and *fbpBC*-bearing transcripts.

The test samples were cDNA primed with random hexamers, and 10-fold serial dilutions of pCR2FABC DNA were employed to generate the standard curves. Kinetic curves are shown for four concentrations of DNA (Fig. 2A and 3A). For each DNA template concentration, a single PCR product of the expected size for primer pairs 560 and 561 and 5′fbpAint and 3′fbpBint was detected by gel electrophoresis, and amplicon fidelity was confirmed by melting curve analysis (data not shown). Each kinetic curve was defined by a cycle threshold value (C_t) which marks the fractional cycle number during the logarithmic phase at which the fluorescence of a given sample becomes significantly different from the baseline signal. The C_t value also represents the crossover point between the kinetic curve and an arbitrary fluorescence level, which for all of the experiments presented is 1.5. C_t values are inversely proportional to the log of the initial template concentration and thus are used to calculate transcript copy number. The target message in the unknown sample is quantified by measuring C_t and by using the calibration curve performed during the same experiment to determine the starting target message quantity. As depicted in the calibration curves for each primer pair (Fig. 2B and 3B), the kinetic PCR assay exhibited a dynamic range of at least 4 orders of magnitude.

These experiments revealed that *fbpA* mRNA was expressed at a 10- to 20-fold-higher level than the *fbpAB* transcript (Fig. 2 and 3). Similar ratios were observed when the level of *fbpA* transcript was compared to that of the *fbpBC*-expressing transcript (data not shown). These results indicate a preferential accumulation of *fbpA* transcript relative to full-length *fbpABC* mRNA.

The evidence provided in this study unequivocally shows that the meningococcal *fbpABC* locus is transcribed as a single contiguous message, and, therefore, this gene cluster is organized as a polycistronic operon. A prior report employing RT-PCR amplification was unable to detect either *fbpC* or *fbpBC* transcripts (25). The reasons for the discordant results are

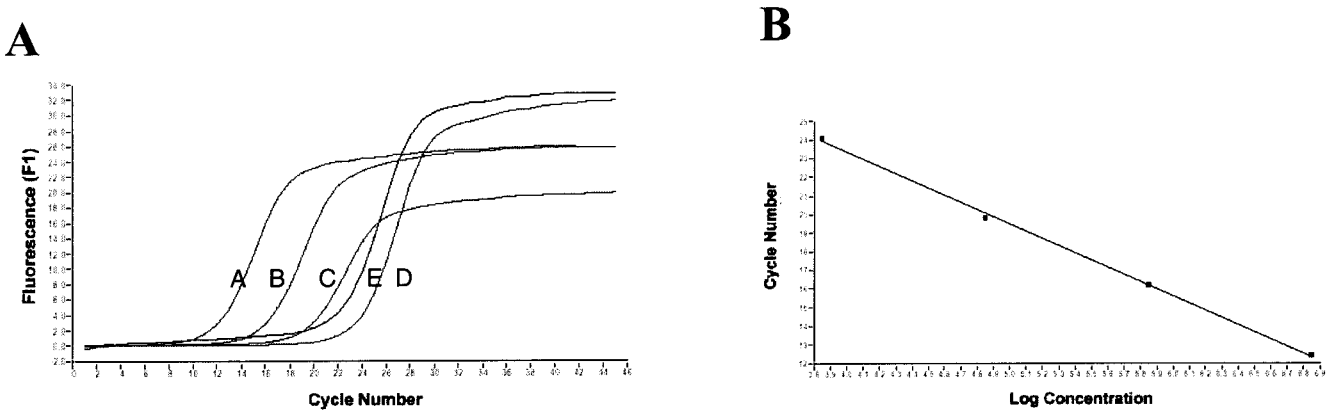

C

Primer pair	Template	Added copy number	Calculated copy number	C_t
fbpAint/fbpBint	pCR2FABC	7,000,000	6,661,000	12.43
fbpAint/fbpBint	pCR2FABC	700,000	695,000	16.23
fbpAint/fbpBint	pCR2FABC	70,000	82,000	19.82
fbpAint/fbpBint	pCR2FABC	7,000	6,294	24.14
fbpAint/fbpBint	Random hexamer primed cDNA	Unknown	13,920	22.81

FIG. 3. (A) Kinetic PCR curves for primer pair 5′fbpAint and 3′fbpBint. Relative fluorescence output is plotted versus PCR cycle number. Kinetic curves are for 10^6 (A), 10^5 (B), 10^4 (C), and 10^3 (D) pCR2FABC DNA template copy numbers and for random hexamer-primed cDNA (E). (B) Calibration curve for primer pair 3′fbpBint. The C_t value from each kinetic curve is plotted versus the log of the initial DNA concentration. (C) Copy number measured by real-time QRT-PCR. The copy number of standard pCR2FABC DNA added to the reactions is calculated from moles of standard pCR2FABC added multiplied by Avogadro's number (6×10^{23}). Given the C_t of each sample, the initial copy number is calculated from the calibration curve conducted during the same experiment. Each assay was performed in triplicate, and representative data from one such experiment are shown. The figure was imaged with a Hewlett-Packard ScanJet HP, edited by using Adobe Photoshop 3.0, and labelled by using Microsoft PowerPoint 97.

unclear, but differences in the primer design and in the RT-PCR amplification protocol represent two potential explanations.

The *fbpAB* and *fbpBC* transcripts detected in this study are likely translationally active, because transcription and translation are coupled processes in prokaryotes. Implicit in this observation is a functional role for both FbpB and FbpC in neisserial periplasmic iron transport from human transferrin and human lactoferrin. However, the mandatory participation of FbpC remains uncertain, because a previous investigation showed that a gonococcal *fbpC* mutant is unimpaired in the ability to access iron from human transferrin and human lactoferrin for growth (25).

There are several possible explanations for this observation, but no version supplies an immediately patent answer. First, functional disruption of *fbpC* may have unmasked the presence of an unidentified subsidiary ABC transporter involved in neisserial periplasmic iron transport. Such an explanation is unlikely, since in an antecedent study, an *fbpABC* mutant, which might also be anticipated to exhibit an iron acquisition phenotype, similar to that of the *fbpC* mutant, is incompetent in iron utilization (14). Second, iron transport in the *fbpC* mutant may have been restored by the presence of another chromosomal wild-type copy of *fbpABC*. The absence of other gonococcal gene loci displaying significant sequence homology to *fbpABC* in an analysis of the assembled contigs deposited in the ongoing gonococcal and meningococcal genome projects renders this explanation unlikely. Third, iron transport in the *fbpC* mutant may have been rescued by complementation with a heterologous ATPase subunit. Such functional exchange has occurred only in the context in which the heterologous complementing ATPase component is significantly overexpressed with respect to its respective cognate integral membrane protein (11, 28). Because this requirement has not been directly satisfied in the defined *fbpC* mutant, this explanation also appears unlikely to apply.

The enhanced amount of the *fbpA*-bearing transcript compared to the full-length *fbpABC* mRNA has several significant implications. First, this result supplies a molecular correlate for the observation that FbpA is synthesized in excess of the permease components FbpB and FbpC (1, 3). A cardinal feature of bacterial binding-protein-dependent importers is the preferential production of the periplasmic binding protein constituent (27). This characteristic is functionally relevant because the efficiency of the transport process is critically dependent upon the preservation of such a stoichiometry (16).

Second, this result suggests that segmental differences in transcript stability may account for the differential expression of individual genes in the *fbpABC* operon. Such differential rates of transcript decay underlie the preferential accumulation of the periplasmic binding protein MalE in the *E. coli* maltose transporter *malEFGK* (7). The increased stability of the *malE* transcript is a consequence of a stem-loop structure located in the *malEF* intergenic region (18, 19). Many stem-loop structures serve as barriers to 3′→5′ exonucleases (13, 19) by impeding the processive action of these enzymes, thereby increasing the chemical longevity of upstream mRNA. The sequence comprising the neisserial *fbpAB* intercistronic junction exhibits the potential to adopt a similar conformation (1), raising the intriguing speculation that this secondary structure represents the structural determinant of *fbpA* transcript stability.

In summary, we have established that the meningococcal *fbpABC* locus exhibits an operonic organization. The genetic (4), structural, and immunological (17) conservation of *fbpABC* in the pathogenic *Neisseria* spp. suggests that the results from this investigation apply to *N. gonorrhoeae*.

This work was supported by a grant (MT-15111) from the Medical Research Council of Canada. V.D. is the recipient of a summer studentship from the Alberta Heritage Foundation for Medical Research.

We thank R. Chalus for excellent technical assistance with the use of the LightCycler Instrument.

REFERENCES

1. **Adhikari, P., S. A. Berish, A. J. Nowalk, K. L. Veraldi, S. A. Morse, and T. A. Mietzner.** 1996. The *fbpABC* locus of *Neisseria gonorrhoeae* functions in the periplasm-to-cytosol transport of iron. J. Bacteriol. **178:**2145–2149.
2. **Ames, G. F.-L.** 1986. Bacterial periplasmic transport systems: structure, mechanism, and evolution. Annu. Rev. Biochem. **55:**397–425.
3. **Berish, S. A., C.-Y. Chen, T. A. Mietzner, and S. A. Morse.** 1992. Expression of a functional neisserial *fbp* gene in *Escherichia coli*. Mol. Microbiol. **6:**2607–2615.
4. **Berish, S. A., D. Kapczunski, and S. A. Morse.** 1990. Nucleotide sequence of the Fbp gene from *Neisseria meningitidis*. Nucleic Acids Res. **18:**4596.
5. **Chen, C.-Y., S. A. Berish, S. A. Morse, and T. A. Mietzner.** 1993. The ferric iron-binding protein of pathogenic *Neisseria* spp. functions as a periplasmic transport protein in iron acquisition from human transferrin. Mol. Microbiol. **10:**311–318.
6. **Doige, C. A., and G. F.-L. Ames.** 1993. ATP-dependent transport systems in bacteria and humans: relevance to cystic fibrosis and multidrug resistance. Annu. Rev. Microbiol. **47:**291–319.
7. **Ehrmann, M., R. Ehrle, E. Hofmann, W. Boos, and A. Schlosser.** 1998. The ABC maltose transporter. Mol. Microbiol. **29:**685–694.
8. **Fleischmann, R. D., M. D. Adams, O. White, E. F. Kirkness, A. R. Kerlavage, C. J. Bult, J. F. Tomb, B. A. Dougherty, J. M. Merrick, et al.** 1995. Whole-genome random sequencing and assembly of *Haemophilus influenzae* Rd. Science **269:**496–512.
9. **Forng, R.-Y., C. R. Ekechukwu, S. Subbarao, S. A. Morse, and C. A. Genco.** 1997. Promoter mapping and transcriptional regulation of the iron-regulated *Neisseria gonorrhoeae fbpA* gene. J. Bacteriol. **179:**3047–3052.
10. **Hatten, L. A., H. P. Schweizer, N. Averill, L. Wang, and A. B. Schryvers.** 1993. Cloning and characterization of the *Neisseria meningitidis asd* gene. Gene **129:**123–128.
11. **Hekstra, D., and J. Tommassen.** 1993. Functional exchangeability of the ABC proteins of the periplasmic binding protein-dependent transport systems Ugp and Mal of *Escherichia coli*. J. Bacteriol. **175:**6546–6552.
12. **Higgins, C. F.** 1992. ABC transporters: from microorganisms to man. Annu. Rev. Cell Biol. **8:**67–113.
13. **Hiles, I. D., M. P. Gallagher, D. J. Jamieson, and C. F. Higgins.** 1987. Molecular characterization of the oligopeptide permease of *Salmonella typhimurium*. J. Mol. Biol. **195:**125–142.
14. **Khun, H. H., S. D. Kirby, and B. C. Lee.** 1998. A *Neisseria meningitidis fbpABC* mutant is incapable of using nonheme iron for growth. Infect. Immun. **66:**2330–2336.
15. **Linton, K. J., and C. F. Higgins.** 1998. The *Escherichia coli* ATP-binding cassette (ABC) proteins. Mol. Microbiol. **28:**5–13.
16. **Mademidis, A., and W. Koster.** 1998. Transport activity of FhuA, FhuC, FhuD, and FhuB derivatives in a system free of polar effects, and stoichiometry of components involved in ferrichrome uptake. Mol. Gen. Genet. **258:**156–165.
17. **Mietzner, T. A., R. C. Barnes, Y. A. Jeanlouis, W. M. Shafer, and S. A. Morse.** 1986. Distribution of an antigenically related iron-regulated protein among the *Neisseria* spp. Infect. Immun. **51:**60–68.
18. **Newbury, S. F., N. H. Smith, and C. F. Higgins.** 1987. Differential mRNA stability controls relative gene expression within a polycistronic operon. Cell **51:**1131–1143.
19. **Newbury, S. F., N. H. Smith, E. C. Robinson, I. D. Hiles, and C. F. Higgins.** 1987. Stabilization of translationally active mRNA by prokaryotic REP sequences. Cell **48:**297–310.
20. **Quiocho, F. A., and P. S. Ledvina.** 1996. Atomic structure and specificity of bacterial periplasmic receptors for active transport and chemotaxis: variation of a common theme. Mol. Microbiol. **20:**17–25.
21. **Sambrook, J., E. F. Fritsch, and T. Maniatis.** 1989. Molecular cloning: a laboratory manual, 2nd ed. Cold Spring Harbor Laboratory Press, Cold Spring Harbor, N.Y.
22. **Sanger, F., S. Nicklen, and A. R. Coulson.** 1977. DNA sequencing with chain terminating inhibitors. Proc. Natl. Acad. Sci. USA **74:**5463–5467.
23. **Saurin, W., and E. Dassa.** 1996. In search of *Mycoplasma genitalium* lost substrate-binding proteins: sequence divergence could be the result of a broader substrate specificity. Mol. Microbiol. **22:**389–390.
24. **Schneider, E., and S. Hunke.** 1998. ATP-binding-cassette (ABC) transport systems: functional and structural aspects of the ATP-hydrolyzing subunits/domains. FEMS Microbiol. Rev. **22:**1–20.
25. **Sebastian, S., and C. A. Genco.** 1999. FbpC is not essential for iron acquisition in *Neisseria gonorrhoeae*. Infect. Immun. **67:**3141–3145.
26. **Tam, R., and M. H. Saier, Jr.** 1993. Structural, functional, and evolutionary relationships among extracellular solute-binding receptors of bacteria. Microbiol. Rev. **57:**320–346.
27. **Torres, A. G., and S. M. Payne.** 1997. Haem iron-transport system in enterohaemorrhagic *Escherichia coli* O157:H7. Mol. Microbiol. **23:**825–833.
28. **Wilken, S., G. Schmees, and E. Schneider.** 1996. A putative helical domain in the Malk subunit of the ATP-binding-cassette transport system for maltose of *Salmonella typhimurium* (MalFGK2) is crucial for the interaction with MalF and MalG. A study using the LacK protein of *Agrobacterium radiobacter* as a tool. Mol. Microbiol. **22:**655–666.
29. **Wittwer, C. T., K. M. Ririe, R. V. Andrew, D. A. David, R. A. Gundry, and U. J. Balis.** 1997. The LightCycler: a microvolume multisample fluorimeter with rapid temperature control. BioTechniques **22:**176–181.

Editor: E. I. Tuomanen